GaN HEMT Device Model Development for Implementation of Different Circuit Designs

Mridula Gupta,
Sr. Professor,
mridula@south.du.ac.in
Department of Electronic Science
University of Delhi South Campus
New Delhi, India.

Abstract

GaN HEMT devices (with different dimensions) have been investigated using 16- and 22-element small-signal equivalent circuit Model. The percentage error is estimated to show the difference in extracted parameters using 16- and 22-element small-signal equivalent circuit model which assist in choosing the accurate small-signal model for large gate periphery GaN HEMTs. For device's low power operation linear models are sufficient. In order to achieve higher certainty for high power applications, the non-linear behaviour of the device must be considered. While generating the large-signal device model, the nonlinear capacitances C_{gs} and C_{gd}, as well as the current source I_{ds} are primarily considered to capture the non-linear behavior of the device. The capacitances, C_{gs} and C_{gd}, are dependent on applied bias i. e. V_{gs} and V_{ds}. The Angelov model for I_{ds} is used to generate the non-linear model parameters which uses the multi-bias small-signal equivalent circuit parameters.

Keywords: HEMT, I-V Characteristc, S-Parameter, 16- and 22-Element Equivalent Circuit Model, Large-Signal Model.

INTRODUCTION

Gallium nitride-based HEMTs (high-electron mobility transistor) provides higher cut-off frequency and higher breakdown voltage and shows outstanding power and frequency performance over the past decade [1] [2]. GaN HEMTs are now the most promising devices for RF switches, low noise amplifiers and power amplifiers, which are essential components of transceiver systems. The need for an accurate device model becomes paramount for the design and analysis of any active circuit. Small-signal equivalent circuit models are adequate for low power operation devices. The non-linear behaviour of the device must be considered in order to obtain high accuracy for high power applications. GaN device modeling has been the subject of numerous reported works. There have been claimed to be several ways to simulate GaN HEMTs, each with advantages and disadvantages [3] [4] [5] [6] [7]. Several large-signal HEMT models (empirical equation based), including the ASM HEMT model [8], Curtice model [9] and Angelov (Chalmers) model [10], have previously been created and integrated with several commercial computer-aided design (CAD) programs. Different formulas are used by these models, based on the I-V characteristics between the subthreshold and saturation area, to fit the electrical behavior of the device.

In this work, the 16- and 22-element small signal model were used for parameters extraction. GaN HEMT devices with Different dimensions have been investigated using these techniques. The device's Stability Factor, K-factor, Maximum Gain and Delta Factor were simulated. The 16- and 22-element small signal equivalent circuit models are compared and the percentage error were estimated to depict the preciseness of 16- and 22-element small signal model to be chosen for large gate perphery devices.
The small model should be accurate, easy to apply in commercial simulators and relatively quick to extract. In this work, the multi-bias small-signal equivalent circuit parameters are extracted which is beneficial in generating the non-linear model of the device.

EXTRACTION METHODOLOGY

Small-signal model of the microwave transistor has been the subject of much debate and is still debated [20-22], due to the interests and challenges this area of research.

The small-signal models often act as the basis of large-signal and noise modelling which provides the main reason for such a great interest. The small-signal equivalent circuits used for the parameter extraction are shown in figure 2 (a) and (b). Figure 2 (a) shows the 16-element circuit consisting of 8 intrinsic and 8 extrinsic parameters and figure 2 (b) shows the 22-element circuit consisting of 10 intrinsic and 12 extrinsic elements. The intrinsic elements are surrounded by the dash lines in

figure 2(a) and (b). These models consider the the parasitic resistances (R_s, R_g and R_d); contact inductances (L_g, L_s and L_d); the gate and drain pad capacitances (C_{pg} and C_{pd}). The C_{gd}, C_{gs} and C_{ds} are the intrinsic capacitances between different contacts (such as gate-drain, gate-source and drain-source). g_d and g_m represents the output and intrinsic transconductances. The channel resistance associated are R_i and R_{gd}. The τ is the time delay i.e. the change of gate voltage w. r. t. drain current. The parasitic pad capacitances were differentiated as 6 different capacitances in 22-element model: C_{pdi}, C_{pgi}, C_{gdi}, C_{pda}, C_{pga} and C_{gda}. G_{gsf} and G_{gdf} models the conduction current through the gate-source and gate-drain terminals. The conventional approach has been considered for extraction of parameters and has been depicted as a flow chart in figure 3. First, the experimental [19] S-parameter at V_{gs}=-5 V and V_{ds}=0 V (cold pinch off condition) is used to estimate the pad capacitances. When determining the parasitic inductances and resistances, V_{gs} and V_{ds} in a cold HEMT measurement, i.e., 0 V. The curve fitting method is then applied to quantify the resistances and inductances. Additionally, the parasitic capacitances and resistance under the gate are considered [12], the extrinsic parameters' fidelity is increased, and this is crucial for the intrinsic parameters to be accurate.

The measured s-parameters are transformed into Z- and Y-parameters at V_{gs}=-3 V and V_{ds} = 10 V, followed by the extrinsic parameters de-embedding, to obtain the intrinsic parameters. These extrinsic and intrinsic parameters are the initial values for the circuit simulation.

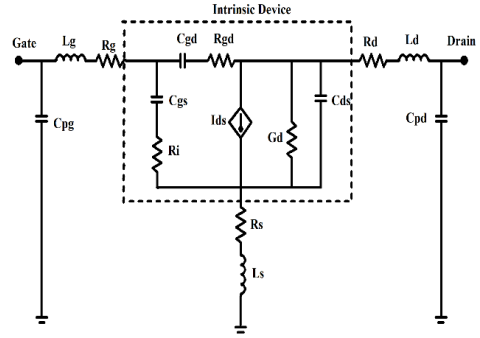

(a)

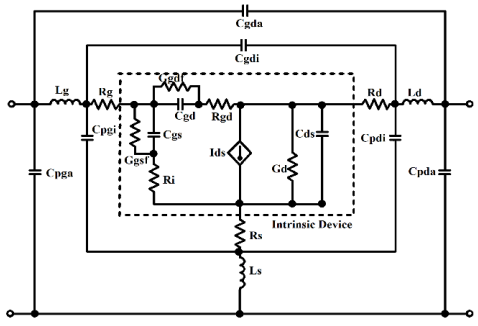

(b)

Fig. 2. (a) 16-Element Small-Signal Equivalent Circuit Model and (b) 22-Element Small-Signal Equivalent Circuit Model.

Subsequent to the extraction small-signal equivalent circuit is designed in ADS software using these parameter initial values followed by the optimization and tuning the parameters to get good congruency between the measured and simulated s-parameters.

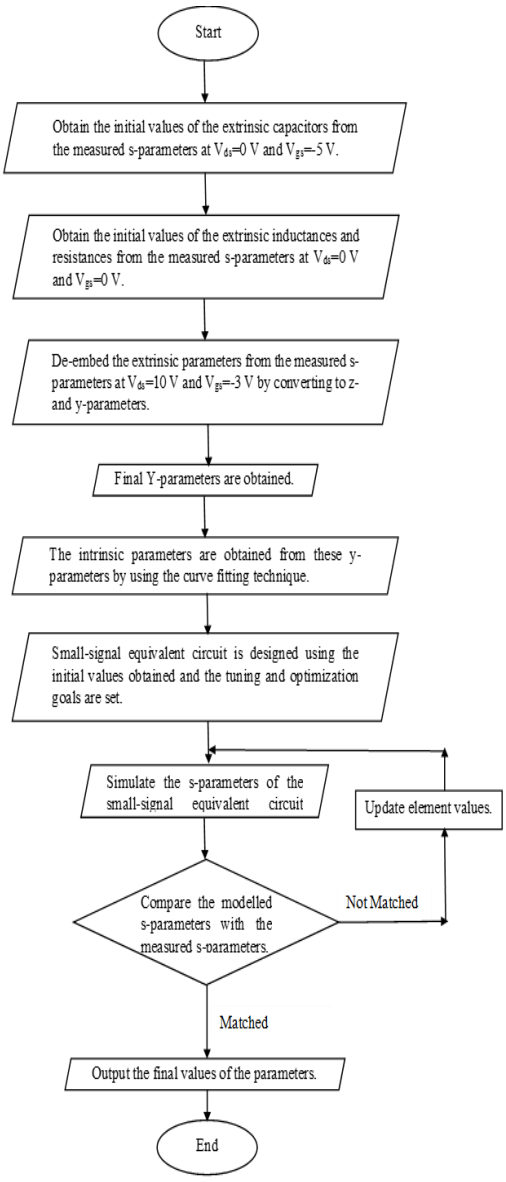

Fig. 3. Flow chart representaton of parameter extracton technque.

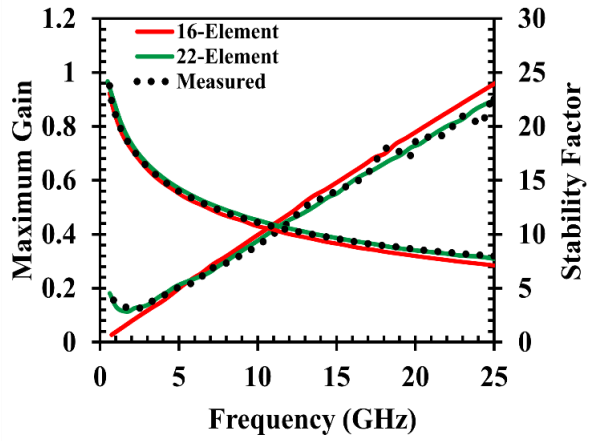

(a)

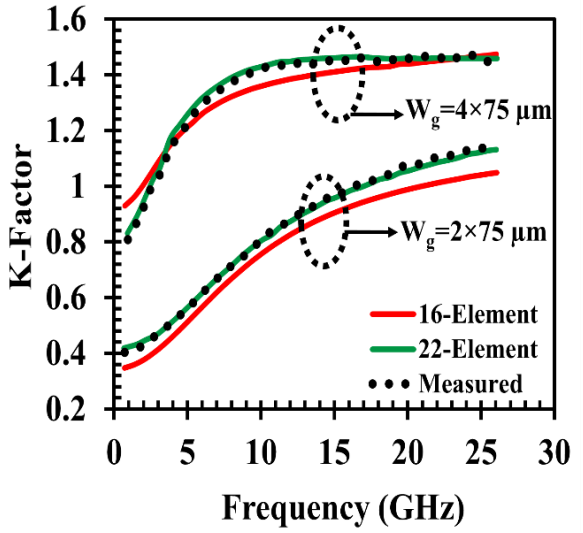

(b)

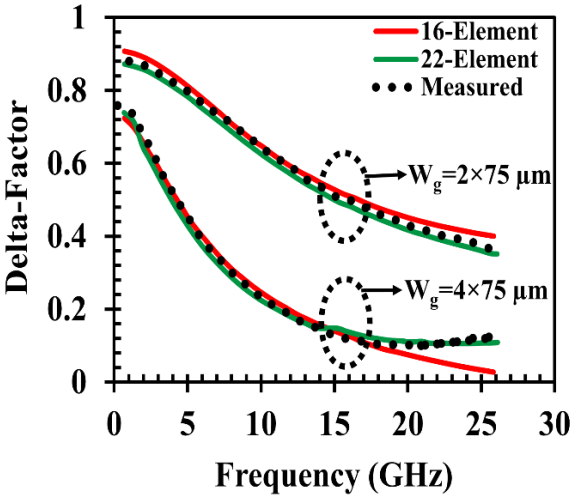

(c)

Fig. 4. Comparison of (a) Maximum Gain and Stability Factor, (b) K-Factor and (c) Delta Factor between the measured, 16- and 22-element small-signal model of GaN HEMT.

RESULTS AND DISCUSSION

Following the extraction procedure, explained by the flow chart in figure 3, the intrinsic and extrinsic parameters were extracted using 16- and 22-element model using the measured s-parameters. The circuit was designed in ADS and S-parameter were simulated (frequency range 500 MHz to 26 GHz). To get a good congruency between the measured and simulated results, the optimization and tuning tools in ADS were used to tune the parameters [19] for both the models. The GaN HEMT devices, having different dimensions, were investigated. After optimization, the Stability Factor, K-factor, Maximum Gain and Delta Factor were simulated using both the models. The Stability Factor, K-factor, Delta Factor and Maximum Gain are represented (in terms of S-parameters) as follows [23]:

$$\textit{Stability Factor} = 1 + |S_{11}|^2 - |S_{22}|^2 - |S_{11}*S_{22} - S_{12}*S_{21}|^2 \quad \text{.....(1)}$$

$$K\text{-}Factor = \{1 - |S_{11}|^2 - |S_{22}|^2 + |\Delta|^2\} / \{2*|S_{12}*S_{21}|\} \quad \text{.....(2)}$$

$$\textit{Delta Factor} = \Delta = S_{11}*S_{22} - S_{12}*S_{21} \quad \text{.....(3)}$$

$$\textit{Max. Gain} = (K - \sqrt{(K^2-1)})*(S_{21}/S_{12}) \quad \text{.....(4)}$$

The results obtained for Stability Factor, K-factor, Maximum Gain and Delta Factor for 16- and 22- element models were compared with the measured data which are depicted in figure 4 (a-c). The % error, depicted in figure 5 (a-d) were calculated between the simulated 16- and 22-element model with measured [19] Stability Factor, K-factor, Maximum Gain and Delta Factor for GaN HEMTs. From figure 5, it can be observed that, as the source to drain distance is increased, the percentage error is reducing for the 22-element model. In case of stability factor the reduction is as following:13.47%–8.11% with difference of 5.36% for L_{sd}=2.5 µm, 13.05%–7.40% with difference of 5.65% for L_{sd}=3.0 µm and 10.42%–4.74% with difference of 5.68% for L_{sd}=4.0 µm. Analogous effect can be observed for the increased number of fingers of the device. Thus can be concluded that the 22-element model gives more accurate small-signal equivalent circuit model for large gate periphery devices [19].

The intrinsic parameters have been extracted for different V_{gs} and V_{ds} as these parameters are bias dependent. The intrinsic parameters were optimized (extrinsic element values were constant). The RF characteristics (fT, fMax., voltage gain, current gain, power gain) of the GaN HEMT are the functions of device intrinsic parameters. The intrinsic parameters of the device are dependent on the gate and drain bias. Hence, the gate and drain bias will affect the RF characteristics (fT, fMax., voltage gain, current gain, power gain) of the GaN HEMT. To show the bias dependency of the intrinsic parameters, the extraction were carried out for different V_{gs} and V_{ds}. Fig. 6 (a-f) represents the intrinsic parameters versus gate bias for different drain bias.

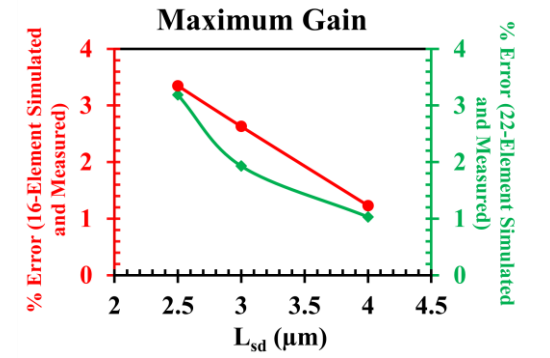

(a)

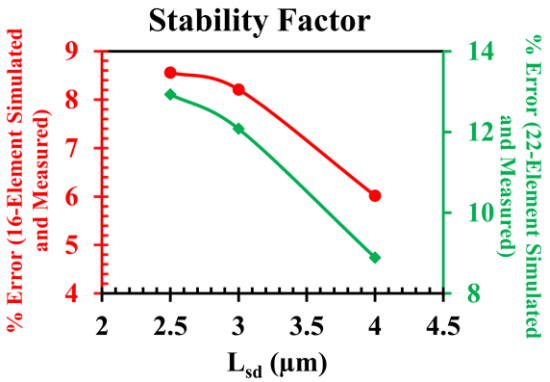

(b)

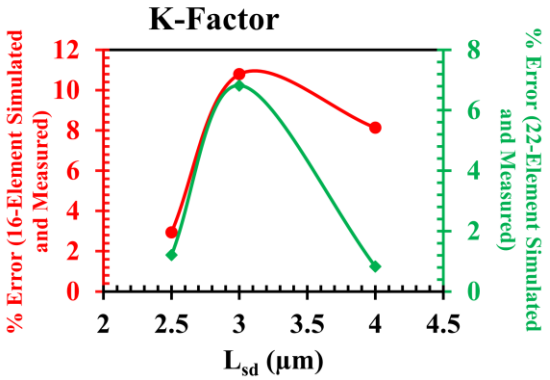

(c)

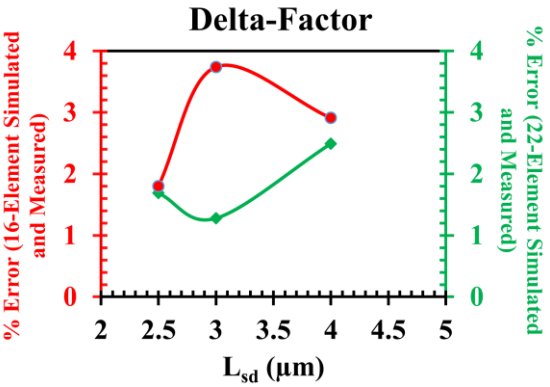

(d)

Fig. 5. The percentage Error Between The 16- And 22-Element Model Simulated with Measured (a) Maximum Gain, (b) Stability Factor, (c) K-Factor and (d) Delta Factor.

The depletion layer behind the gate controls the capacitance (C_{gs}) between the gate metal and channel charge in 2DEG. When V_{gs} rises from the pinchoff region, C_{gs} rises as well. Beyond a certain voltage, the drain current saturates as V_{gs} rises, and the depletion area stops changing. C_{gs} and V_{gs} become constant at that voltage. The drain voltage creates a lateral electric field that accelerates the channel's carriers. As a result, the depletion layer depth is decreased, which leads to a modest increase in C_{gs} with V_{ds}. The extended depletion region in the gate-drain area is the cause of C_{gd}. This depletion area widens as the drain voltage rises. As a result, a slight rise in C_{gd} with rising V_{ds} can be seen. A collapse follows a strong increase in the G_m-V_{gs} characteristic that occurs above pinch-off voltage which can be observed in figure 6(c).

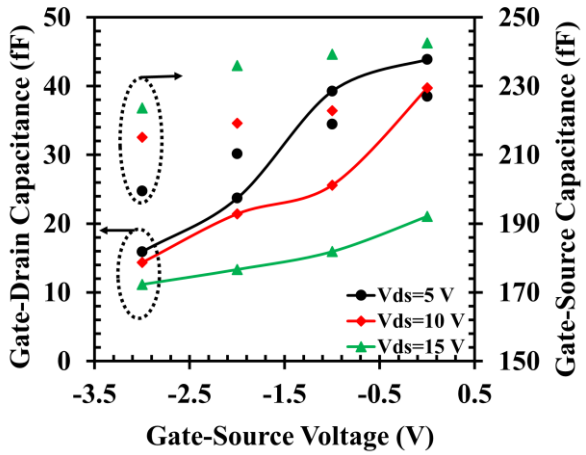

(a)

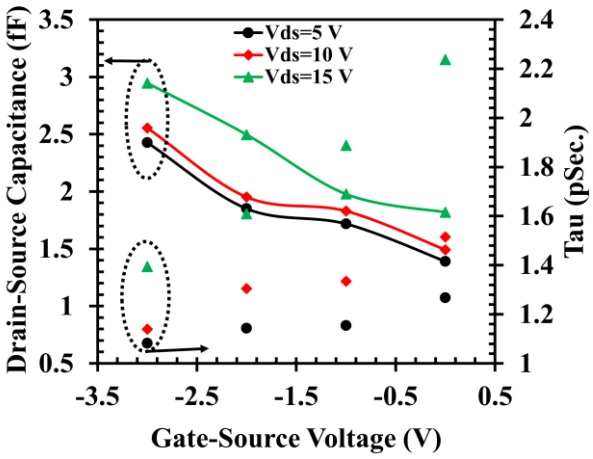

(b)

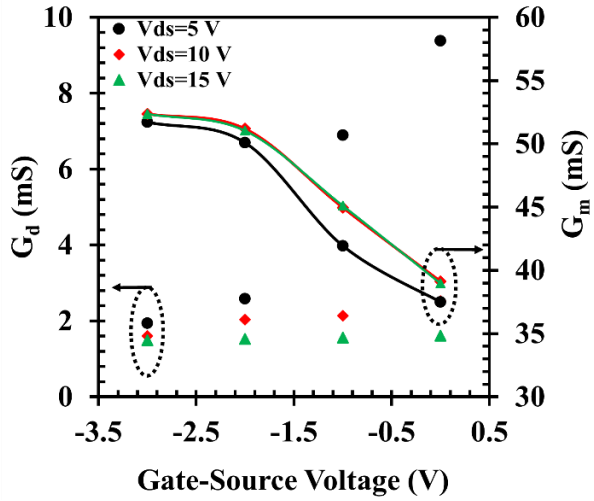

(c)

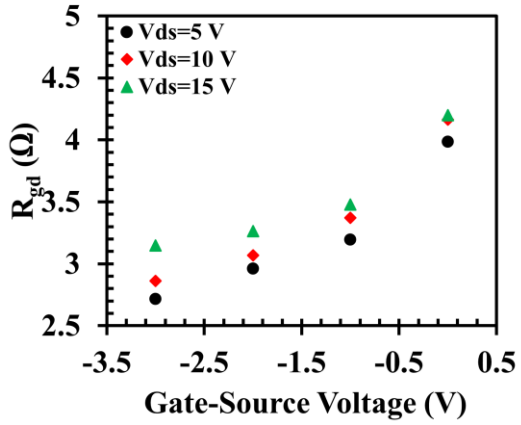

(d)

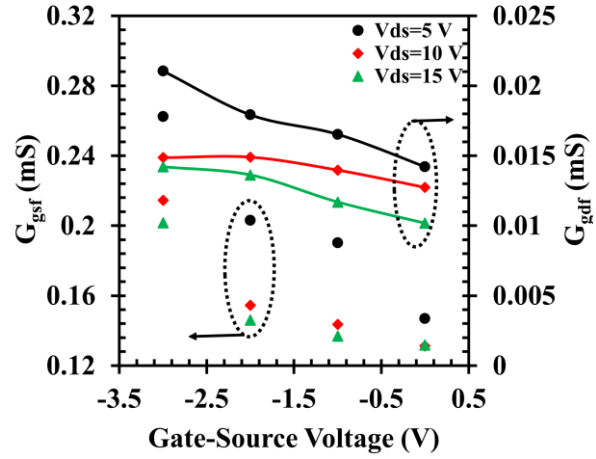

(e)

Due to the abrupt increase in current with V_{ds}, G_d grows with V_{gs} at low V_{ds}. However, in the saturation zone, G_d is minimal. With V_{gs} and V_{ds}, R_i and R_{gd} rise. The transit time for the electrons grows longer as the depletion zone spreads in the gate-drain region. As a result, rises with V_{gs} and Vds.

After the multibias linear model extraction, the non-linear model of the device can be developed. While generating the large-signal model, the non-linear

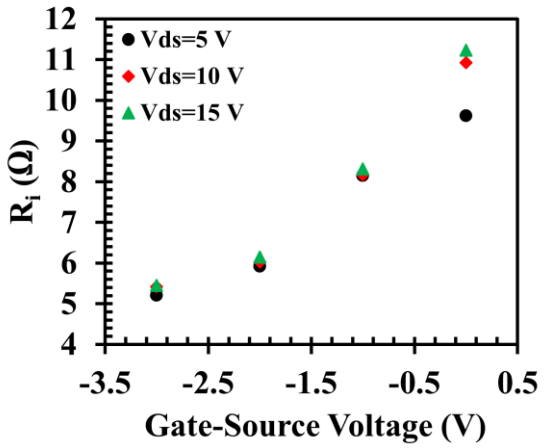

(f)

Fig. 6. Bias dependent intrinsic parameters for GaN HEMT with 0.4 µm gate length and source to drain length 2.5 µm.

behavior of the device must be captured. Hence, the nonlinear capacitances C_{gs} and C_{gd}, as well as the current source I_{ds}, are primarily considered. The current source (I_{ds}) demonstrates the electrical performance of HEMT, which is controlled by Gate voltage and drain voltage. The I-V characteristic of the device can be accurately modeled using this non-linear current source.

CONCLUSION

The findings from the 22-element model demonstrate strong correlation and fewer percentage mismatch with the measured data. The devices with large gate periphery show high accuracy. Hence, the 22-element model gives more accurate small-signal equivalent circuit model for large gate periphery devices. The large-signal model for GaN HEMT device can be generated for further circuit design implimentations with precision to measured results using the multi-bias small-signal equivalent circuit parameters.

ACKNOWLEDGEMENT

The author would like to acknowledge Department of Electronic Science, University of Delhi; Solid State Physics Laboratory, DRDO, Ministry of Defence; DBT STAR College Laboratory at Deen Dayal Upadhyaya College, University of Delhi; Department of Science and Technology and University of Delhi IoE Grant.

REFERENCES

[1] Mishra, U.K., Parikh, P. and Wu, Y.F.: AlGaN/GaN HEMTs-an overview of device operation and applications, in Proceedings of the IEEE, vol. 90, no. 6, pp. 1022-1031, June 2002.

[2] Trew, R.J.: Wide Bandgap Semiconductor Transistors for Microwave Power Amplifiers, IEEE Microwave Magazine, **1**, 2002, 46-54.

[3] Zampardi, P.J. and Kharabi, F.: Industrial view of III–V devices compact modeling for circuit design, IEEE Trans. Electron Devices, **66**, 2019, 28–33.

[4] Liu, L.S., Ma, J.S. and Ng, G.I.: Electrothermal large-signal model of III–V FETs including frequency dispersion and charge conservation, IEEE Trans. Microw. Theory Techn., **57**, 2009, 3106–17.

[5] Angelov, I.: Large-signal modelling and comparison of AlGaN/GaN HEMTs and SiC MESFETs, Proc. Asia–Pacific Microw. Conf., 2006, 279–282.

[6] Avolio, G.: Millimeter-wave FET nonlinear modelling based on the dynamic-bias measurement technique, IEEE Trans. Microw. Theory Techn., **62**, 2014, 2526–37.

[7] Tanimoto, T.: Analytical nonlinear HEMT model for large signal circuit simulation, IEEE Trans. Microw. Theory Techn., **44**, 1996, 1584–6.

[8] Dasgupta, A., Ghosh, S., Chauhan, Y.S. and Khandelwal, S.: ASM-HEMT: Compact model for GaN HEMTs, IEEE International Conference on Electron Devices and Solid-State Circuits (EDSSC), 2015, 495-8.

[9] Curtice, W.R. and Ettenberg, M.: A nonlinear GaAs FET model for use in the design of output circuits for power amplifiers, IEEE MTT-S Int. Microw. Symp. Dig., 1985, 405–8.

[10] Angelov, I., Bengtsson, L. and Garcia, M.: Extensions of the Chalmers nonlinear HEMT and MESFET model, IEEE Trans. Microw. Theory Techn., **44**, 1996, 1664–74.

[11] Dambrine, G., Cappy, A., Heliodore, F. And Playez, E.: A new method for determining the FET small-signal equivalent circuit, IEEE Transactions on Microwave Theory and Techniques, **36**, 1998, 1151-9.

[12] Miras, A. and Legros, E.: Very high frequency small-signal equivalent circuit for short gate-length InP HEMTs, IEEE Trans. Microw. Theor. Tech., **45**, 1997, 1018–26.

[13] Huang, A., Zhong, Z., Guo, Y. and Wu, W.: A new extraction method of extrinsic elements of GaAs/GaN HEMTs, IEEE International Symposium on Radio-Frequency Integration Technology, 2014, 1–3.

[14] Lu, J., Wang, Y., Ma, L. and Yu, Z.: A new small-signal modeling and extraction method in AlGaN/GaN HEMTs, Solid State Electronics, **52**, 2008, 115–20.

[15] Jarndal, A.H. and Kompa, G.: An accurate small-signal model for AlGaN-GaN HEMT suitable for scalable large-signal model construction, IEEE Microw. Wireless Compon. Lett., **16,** 2006, 333–5.

[16] Crupi, G.: Accurate multibias equivalent-circuit extraction for GaN HEMTs, IEEE Trans. Microw. Theory Techn., **54**, 2006, 3616–22.

[17] Zhang, M., Che, W. and Ma, K.: A novel hybrid method for estimating channel temperature and extracting the AlGaN/GaN HEMTs model parameters, IEEE Trans. Electron Devices, **65**, 2018, 1340–7.

[18] Angelov, I., Thorsell, M., Gavel, M. and Barrera, O.: On the modeling of high power FET transistors, Proc. 11th Eur. Microw. Integr. Circuits Conf. (EuMIC), 2016, 245–8.

[19] Anand, A., Rawal, D.S., Narang, R., Mishra, M., Saxena, M. and Gupta, M.: A comparative study on the accuracy of small-signal equivalent circuit modelling for large gate periphery GaN HEMT with diferent source to drain length and gate width, Microelectronics Journal, **118**, 2021, 105258.

[20] Flores, J.A.Z. and Kompa, G.: Closed-form extraction strategy of physically meaningful parameters of small-signal HEMT models with distributed parasitic capacitive effects, IEEE Trans. Microw. Theory Techn., **69**, Feb. 2021, 1227–37.

[21] Colangeli, S.: Nondestructive, self-contained extraction method of parasitic resistances in HEMT devices, IEEE Trans. Microw. Theory Techn., **68**, Jul. 2020, 2571–8.

[22] Jarndal, A., Crupi, G., Raffo, A., Vadalà, V. and Vannini, G.: An Improved Transistor Modeling Methodology Exploiting the Quasi-Static Approximation, IEEE Journal of the Electron Devices Society, **9**, 2021, 378-86.

[23] Keysight Technologies, "Advanced Design System User Manual," Software Manual, 2020.